Recent mechanistic developments for cytochrome *c* nitrite reductase, the key enzyme in the dissimilatory nitrate reduction to ammonium pathway

Krystina Hird*[1], Julius O. Campeciño*[1], Nicolai Lehnert[2], Eric L. Hegg[†1]

[1]Department of Biochemistry & Molecular Biology, Michigan State University, East Lansing, Michigan, USA

[2]Department of Chemistry, University of Michigan, Ann Arbor, Michigan, USA

[†]Corresponding author: Eric Hegg, erichegg@msu.edu; 603 Wilson Rd, East Lansing, MI 48824

*Authors contributed equally

Recent Mechanistic Developments for Cytochrome *c* Nitrite Reductase, the Key Enzyme in the Dissimilatory Nitrate Reduction to Ammonium Pathway

Abstract

Cytochrome *c* nitrite reductase, NrfA, is a soluble, periplasmic pentaheme cytochrome responsible for the reduction of nitrite to ammonium in the Dissimilatory Nitrate Reduction to Ammonium (DNRA) pathway, a vital reaction in the global nitrogen cycle. NrfA catalyzes this six-electron and eight-proton reduction of nitrite at a single active site with the help of its quinol oxidase partners. In this review, we summarize the latest progress in elucidating the reaction mechanism of ammonia production, including new findings about the active site architecture of NrfA, as well as recent results that elucidate electron transfer and storage in the pentaheme scaffold of this enzyme.

Keywords: NrfA; cytochrome *c* nitrite reductase; dissimilatory nitrate reduction to ammonium (DNRA); mechanism; pentaheme; crystal structure

Introduction

Nitrogen is an essential element for all organisms. The most abundant form of nitrogen is atmospheric N_2, which must first be fixed using either an abiotic or a biological energy-intensive process before it is bioavailable. Unfortunately, almost half of the fixed nitrogen that reaches

agricultural lands as fertilizer is lost through biological and physical processes *(1-4)*. Many soil microorganisms readily oxidize ammonium (NH_4^+) either via the comammox (complete ammonia oxidation) or nitrification pathways to nitrite (NO_2^-) and nitrate (NO_3^-), both of which can easily leach from soils and contribute to water pollution and devastating algal blooms (Figure 1). NO_3^- and NO_2^- can also go through denitrification and be lost from the soil via the formation of N_2 or the gaseous intermediates NO and N_2O. Furthermore, fixed nitrogen can be lost as N_2 when NH_4^+ and NO_2^- react in a comproportionating process known as anammox (anaerobic ammonia oxidation).

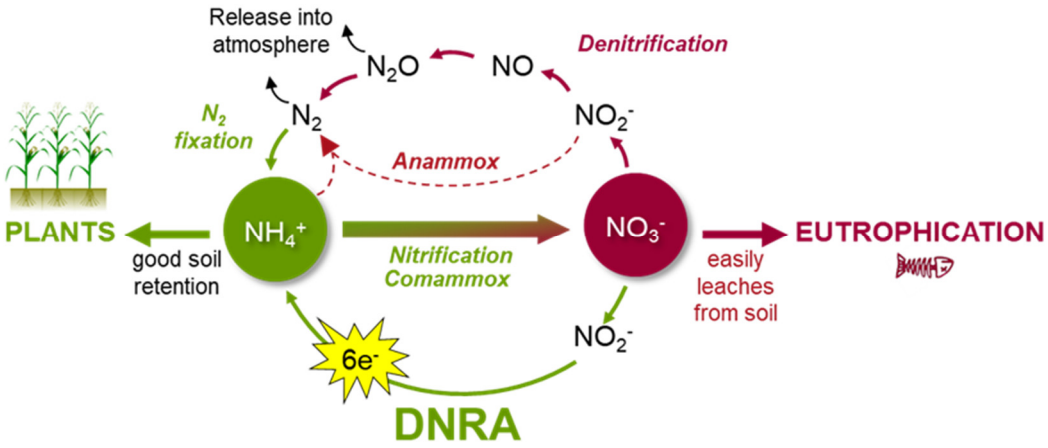

Figure 1. Schematic representation of the nitrification, comammox, anammox, denitrification, and DNRA pathways, adapted from *(5)*.

The Dissimilatory Nitrate Reduction to Ammonium (DNRA) pathway helps retain fixed nitrogen in the soil *(6-12)*. In this pathway, NO_3^- is reduced to NO_2^- in the first step and then further reduced to NH_4^+ in the second step, bypassing the processes of denitrification and nitrogen fixation *(13)*. The pentaheme enzyme cytochrome *c* nitrite reductase, NrfA, is responsible for this second step in an impressive six-electron reduction that occurs at a single

active site *(8, 14, 15)*. The soluble, periplasmic enzyme reaches *in vitro* specific activities of over 1000 µmol NO_2^- min^{-1} mg^{-1} depending on the electron donor *(16-19)*.

There are two main types of NrfA-containing operons found in nature: *nrfHA* and *nrfABCDEFG* (Figure 2). NrfH and NrfB are the redox partners to NrfA in their respective systems *(20)*. In the first system, NrfH transfers electrons from the membrane quinol pool to NrfA while in the second system, a NrfCD complex transfers electrons from the quinol pool to NrfB, which then shuttles the electrons to NrfA *(21)*.

Figure 2. Organization of the *nrfHA* and *nrfABCDEFG* operons, adapted from *(11)*.

Although elucidating the architecture of the Nrf complexes has increased our understanding of electron movement during the DNRA reaction, the nature of the active complex and the physiological relevance of these protein-protein interactions remain largely unknown. The only crystal structure of a NrfAH complex to date, from *Desulfovibrio vulgaris*, reveals an unexpected [NrfA]:[NrfH] ratio of 2:1, resulting in NrfH binding asymmetrically at the NrfA-NrfA dimer interface. It is unknown if this binding arrangement can be extended to other organisms, but if this structure is physiologically relevant, then NrfH can only deliver electrons to one of the two NrfA enzymes. Dynamic light scattering data with purified NrfA, however, indicate that the enzyme may function as a monomer rather than a dimer in some organisms *(16, 22)*, although it is also possible that NrfA requires contact with its redox partner to form a stable,

functional NrfA dimer. Furthermore, the storage and movement of electrons by NrfA and its corresponding redox partners are critical to the function of these complexes, but the mechanism by which electron transfer occurs and is regulated is still not fully understood. This article reviews the latest findings on the coordinated flow of electrons in NrfA, the proposed mechanism of the intriguing reaction that this enzyme catalyzes, and the structure-function relationships of NrfA.

Structure of NrfA

All available crystallographic data of NrfA (Table 1) display a dimeric structure that has generally been assumed to be the functional unit of this enzyme (Figure 3) *(14, 16, 18, 23-29)*. The dimer interface is dominated by the three main α-helices from each monomer and is stabilized by both salt bridges and other H-bonding interactions. Each monomer contains five *c*-type hemes *(13, 30)*, and these hemes are numbered according to the position of their binding sites in the polypeptide chain. Hemes 1, 3, and 4 are coplanar and are believed to be involved in π-stacking interactions *(13, 30)*. Heme 2 is perpendicular to heme 3 and is likely the entry point of electrons into NrfA, while heme 5 is perpendicular to heme 4 and sits at the dimer interface (Figure 4). Hemes 2-5 are bound to canonical CXXCH motifs and are low-spin bis-His ligated. The catalytic site (heme 1), however, is generally bound to a CXXCK motif *(20)*. In the CXXCK motif, the active site heme Fe is in a high-spin resting state and is coordinated by the lysine residue from the motif on the proximal side and a water molecule on the distal side of the heme *(23, 25, 27, 31-33)*.

Table 1. Organisms that have had NrfA structurally characterized.

Proteobacterial clade	Organism	Protein Data Bank
epsilon	*Sulfurospirillum deleyianum*	1QDB *(24)*
	Wolinella succinogenes	1FS7 *(27)*
delta	*Desulfovibrio desulfuricans*	1OAH *(34)*
	Desulfovibrio vulgaris	2J7A *(26)*
	Geobacter lovleyi	6V0A *(16)*
	Geobacter metallireducens	8BCX *(29)*
gamma	*Shewanella oneidensis*	3UBR *(28)*
	Escherichia coli	2RDZ *(25)*

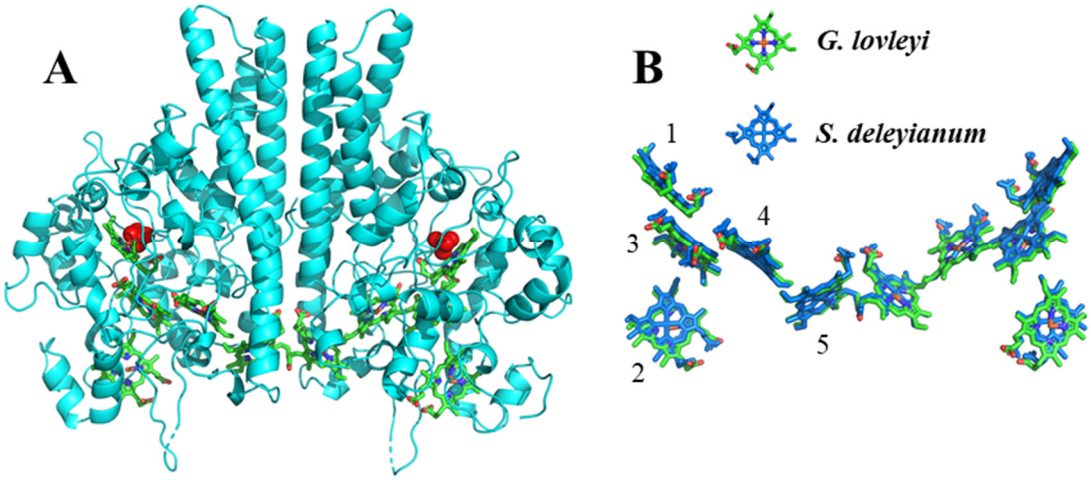

Figure 3. Crystal Structure of *Geobacter lovelyi* NrfA dimer (A) with its hemes (green). Alignment of heme groups (B) from *Sulfurospirillum deleyianum* (PDB: 1QDB) and *G. lovleyi* (PDB: 6V0A). Hemes 1 to 5 are labeled on one of the monomers. The red spheres in the distal position of the active site hemes are sulfate molecules from the crystallization buffer. Figure adapted from *(16)*. (For interpretation of the references to color in this figure legend, the reader is referred to the web version of this article.)

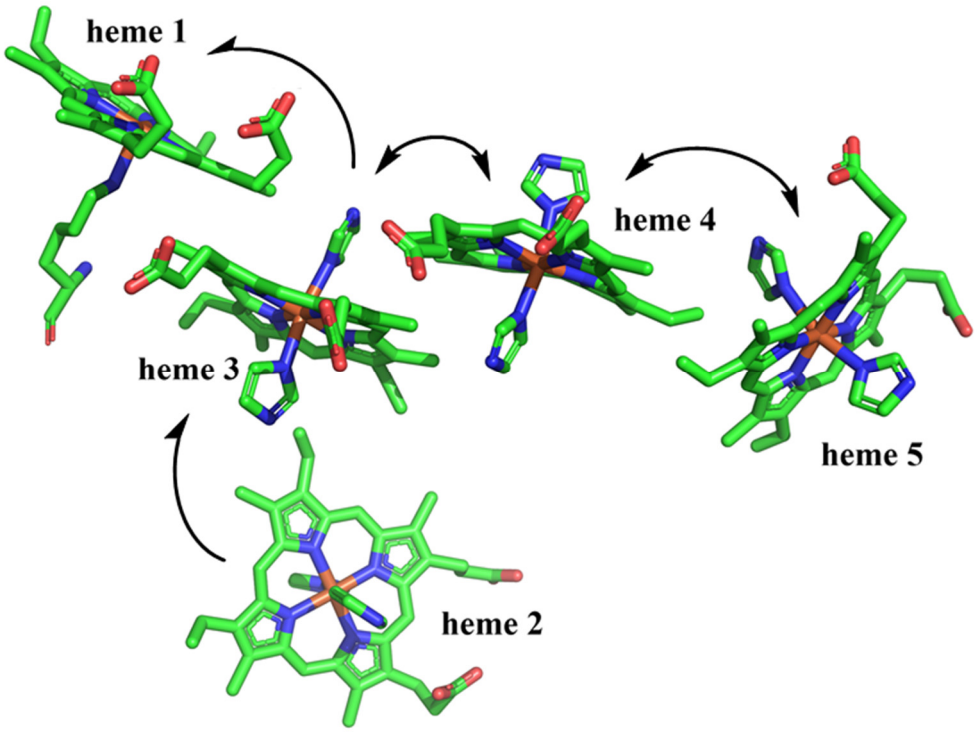

Figure 4. *G. lovleyi* hemes (PDB: 6V0A) shown with the putative flow of electrons and heme-ligand coordination.

The active site has at least three highly conserved second coordination sphere residues: a tyrosine, a histidine, and an arginine. These residues are believed to be involved in proton transport/transfer, substrate delivery, substrate binding, and/or substrate activation *(24-27, 34, 35)*, and we go into greater detail on the catalytic function of these residues in a later section. The second coordination sphere arginine also contributes positive charge to a substrate channel (Figure 5) that leads directly into the active site *(16, 24, 27, 29)*. The inlet of this channel is highly positively charged due to the presence of multiple lysine and arginine residues, which are believed to help deliver nitrite to the active site via electrostatic interaction. The purported channel outlet is highly negatively charged due to the presence of glutamate and aspartate

residues, presumably facilitating the exit of the ammonium product out of the active site *(16, 24, 27, 29)*.

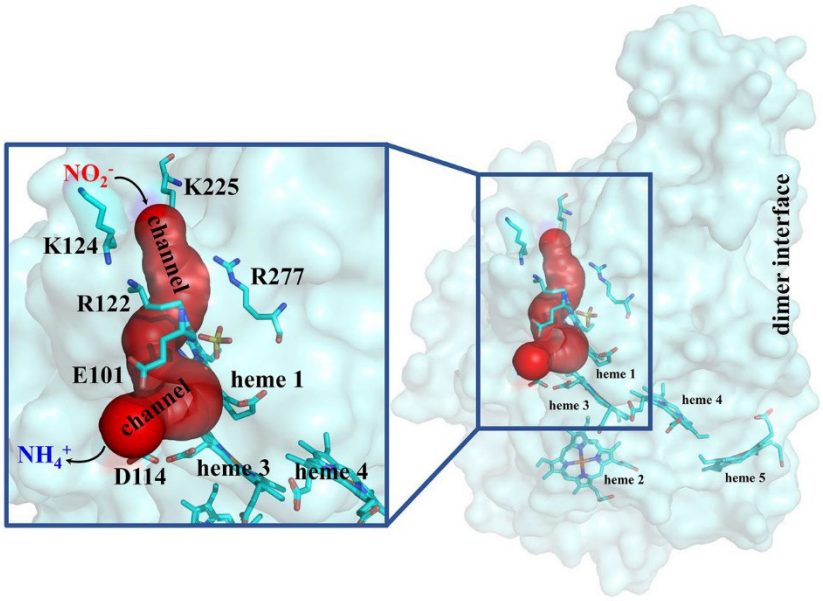

Figure 5. *G. lovleyi* NrfA monomer shown with a putative channel for substrate entry and product exit. Figure from *(16)*.

A critical component of the active site architecture is the presence of a nearby calcium ion (Figure 6A). Removal of the calcium ion by ethylenediaminetetraacetic acid (EDTA) led to a 50% loss of specific activity *(18)*, suggesting an important mechanistic or structural role. There are several hypothesized roles for this active site calcium ion. Firstly, the ion may be necessary for orienting the active site residues. One of the calcium ligands is a glutamine residue that is contiguous to the active site histidine. Ligation of this glutamine residue to the calcium ion effectively inhibits the histidine from binding to the distal side of heme 1, thereby leaving it available to bind substrate *(34)*. The calcium also binds the amide oxygen of the active site tyrosine and may, in effect, help position this residue within the active site *(11)*. Secondly, the calcium ion may also be important for drawing the negatively charged substrate into the active

site via the calcium's positive electrostatic potential. Finally, the calcium has also been postulated to be involved in proton delivery via its two ligating water molecules *(36)*. One homolog of NrfA was found to possess a second calcium ion in the crystal structure *(34)*. This second calcium is octahedrally coordinated like the active site calcium ion, but this second calcium ion utilizes the propionate groups from heme 3 and 4 for coordination. The physiological significance of the second calcium remains to be elucidated.

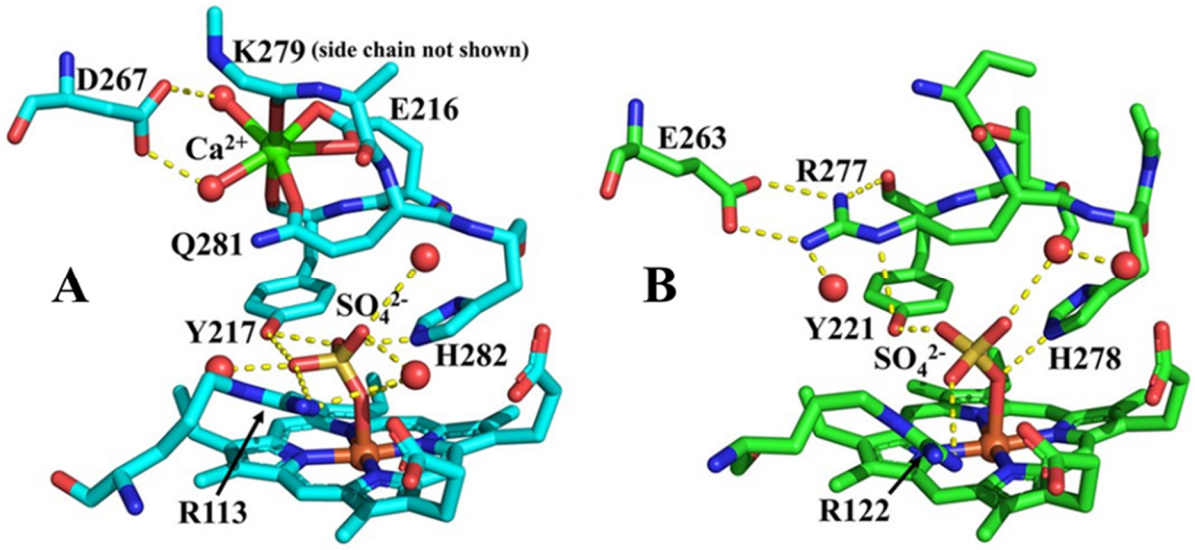

Figure 6. Active site structure of *S. deleyianum* NrfA (A) and *G. lovleyi* NrfA (B). *S. deleyianum*'s NrfA is a close homolog of the NrfA from *G. lovleyi (16)*. Figure adapted from *(16)*.

A novel subclass of NrfA was first isolated and characterized from *Geobacter lovleyi (16)* and subsequently characterized from *Geobacter metallireducens (29)*. This homolog shares very similar kinetic, spectroscopic, and structural properties as other characterized NrfA enzymes. However, it exhibits unique features. For instance, although both *Geobacter* enzymes crystallize as dimers, it was found that both purify as monomers *(16, 29)*, even up to an enzyme

concentration of ~300 μM in the case of *G. lovleyi* NrfA. This observation contrasts with what has been found for the *Escherichia coli* NrfA, where the enzyme forms the dimer even at 9 μM concentration *(37)*. It should be noted, however, that both *E. coli* and *G. lovleyi* dimerization studies were performed in the absence of the NrfA redox partners (NrfB and NrfH, respectively). *G. lovleyi*'s NrfH binds tightly to the NrfA dimer at the base of the dimer interface *(26, 31)*, and it stands to reason that if the dimer is the physiologically relevant structure, then NrfA may require NrfH to hold the dimer together. NrfA would therefore exist as a monomer in solution in the absence of its redox partner. Conversely, *E. coli*'s NrfB binds to NrfA away from the dimer interface *(38, 39)*, and therefore the physiological behavior of this NrfA dimer may be mostly independent of the presence of its redox partner.

In addition to the apparent preference of *Geobacter* NrfA for the monomeric state, the enzymes also lack a calcium ion at their active sites. Instead, an arginine bridged to a glutamate is found in the same region as the calcium, and the Arg appears to have similar functionality as the calcium (Figure 6B). For example, the Arg is contiguous to the histidine at the active site and is involved in a hydrogen bonding network that also includes the active site tyrosine. In this way, the Arg helps stabilize the position of the Tyr and His active site residues, which may explain why substitution of this Arg residue in *G. lovleyi* NrfA to alanine, glutamine, or lysine effectively renders the enzyme inactive *(16)*. In addition, a nearby water molecule, albeit only found in two of the six asymmetric units in the *G. lovleyi* crystal structure, is H-bonded with this Arg residue, hinting that the Arg may be involved in delivering protons to the active site. Phylogenetic analysis found that calcium-independent NrfA enzymes only use arginine as a replacement of the ion *(16)*, rather than the positively charged lysine or other amino acids that could also act as proton donors. These functional similarities between the active site calcium of

the canonical NrfAs and the similarly positioned active site Arg of the novel NrfAs provide opportunities for the elucidation of their exact roles in catalysis.

Flow of electrons in NrfA

While it is well established that heme 1 in NrfA is the active site, the remaining hemes are presumably involved in delivering reducing equivalents to the active site and/or storing the necessary reducing equivalents. The arrangement of the hemes in the dimeric structure of NrfA suggests heme 2 as the entry point for the reducing equivalents into the system while heme 5 may serve as a possible relay heme for distributing the reducing equivalents between the two monomers if the dimer is the functional unit (Figure 3). If the monomer is the physiologically functional unit, however, then heme 5 and heme 4 may together be used as electron storage. These electrons could be used later if the flow of electrons from the quinol pool ever becomes limiting. These two possible roles for heme 5 are not mutually exclusive.

To understand the electron flow through NrfA, heme redox potentials were assigned by utilizing the almost unique EPR signatures of the hemes in tandem with cyclic voltammetry experiments *(25, 28, 40-42)*. The assignments were possible because characteristic ferric heme EPR signals ($S = ½$) are well-established in the literature. For instance, bis-His ligated hemes with parallel (*i.e.*, heme 2) or perpendicular (*i.e.*, heme 4) His imidazole plane orientations (Figure 4) are expected to produce either rhombic EPR signals or what is known as "large g_{max}" signals, respectively *(43)*. In addition, while the signals from heme 2 are rhombic and are found below g = 3 (Table 2), those of heme 3 are not observed in the fully oxidized enzyme because this heme is magnetically coupled to heme 1 and heme 4. The signals from heme 3 readily appear, however, upon the reduction of heme 1. The signals from the magnetic coupling of heme

1, heme 3, and/or heme 4 are identified by taking advantage of the fact that heme 1 transitions from high-spin to low-spin upon the binding of a strong-field ligand, *e.g.*, cyanide *(41, 42, 44-46)*.

Table 2. Summary of EPR spectral assignments for NrfA from various organisms. The values listed were reproduced directly from the given reference.

Hemes	*E. coli* NrfA *(25)*	*Shewanella oneidensis* Nrfa *(41)*	*G. lovleyi* NrfA *(42)*
heme 1 (H1)	unassigned	unassigned	2, 2, 2 [a]
heme 2 (H2)	2.92, 2.3, & 1.5	2.94, 2.29, & 1.52	3.01, 2.21, & 1.52
heme 3 (H3)	unassigned	3.07, 2.25, & 1.31	3.22, 2.2, and 1.41
heme 4 (H4)	3.17*	3.39*	3.7 (simulation)
heme 5 (H5)	3.17*	3.39*	3.28 (simulation)
heme coupling (1, 3 and/or 4)	10.8 and 3.5	> 10 and 2.87	10, 3.6, 2.6, & 1.70

*Ambiguous whether signals are from hemes 4 or 5.
[a]High-spin ferric (S = 5/2) ground state

Except for hemes 2 and 3, however, the other signals were difficult to assign unequivocally due to overlapping signals and electronic coupling. With the aid of simulations, however, Sosa *et al.* unraveled these ambiguous signals *(42)*. Additional confirmations of the assignments of the EPR signals to individual hemes were achieved using site-directed mutagenesis to substitute the distal His ligand of hemes 3 and 5 to Met *(41, 42)*. A summary of the EPR spectral assignments is provided in Table 2.

With the heme EPR signature assignments established, the assignment of the heme redox potentials should in theory be relatively straightforward. First, the order of heme reductions was identified by following the successive disappearance of the EPR signatures as the enzyme was electrochemically or chemically reduced. Midpoint potentials obtained either from non-turnover

protein-film voltammetry *(28, 42, 47)*, EPR *(40)*, UV-Vis *(28, 41)*, or magnetic circular dichroism (MCD) *(40)* spectropotentiometry were then simply assigned to each heme according to the order of their reduction. These assignments are summarized in Table 3.

Table 3. Heme redox potentials of NrfA from different organisms.

S. oneidensis (41) WT NrfA (mV)	*G. lovleyi (42)* WT NrfA (mV)	*G. lovleyi (42)* H108M* NrfA (mV)
−44 ± 2 (H1)	+10 ± 2 (H4/H5)	+48 ± 8 (H3)
−110 ± 4 (H4)	−66 ± 11 (H4/H5)	−24 ± 17 (H4)
−210 ± 20 (H2)	−152 ± 27 (H1)	−103 ± 22 (H5)
−257 ± 17 (H5)	−180 ± 10 (H2)	−160 ± 13 (H1)
−382 ± 4 (H3)	−226 ± 7 (H3)	−210 ± 9 (H2)

*The heme 3 ligand, His108, was replaced with Met.

Despite the rigorous and careful assignments of heme EPR signals by the various research groups, there is no consensus as to which heme is reduced first, although this variation could easily be explained by homolog-specific differences or by differences in the experimental techniques employed. Bamford *et al.* (*E. coli*) *(25)* and Stein *et al.* (*S. oneidensis*) *(41)* concluded that heme 1 is reduced first while Marritt *et al.* (*E. coli*) *(40)* saw heme 1 reduced second and Sosa *et al.* (*G. lovleyi*) *(42)* found heme 1 was reduced third. Youngblut *et al.* (*S. oneidensis*) *(48)* proposed a third option, postulating the electrons may be shared among the hemes rather than reducing single hemes.

It is interesting to note that although both Sosa and Stein observed that the first redox equivalent caused an attenuation of the EPR signal at g = ~3.4, different interpretations for this signal attenuation were provided. Stein *et al. (41)* interpreted this as the reduction of heme 1, while Sosa *et al. (42)* interpreted this as the reduction of either heme 4 or 5 (Table 2). It is worth noting that both groups found heme 3 to be magnetically coupled to heme 4, a coupling that was not initially identified. This observation is not surprising given that hemes 3 and 4, like hemes 1 and 3, are sufficiently close to engage in π-stacking interactions *(24, 42)*.

Based on the results from Sosa *et al*., it appears that in *G. lovleyi* NrfA, hemes 4 and 5 are reduced first before heme 1 *(42)*. The authors posited that hemes 4 and 5 may serve as electron storage units, whereby catalysis is not initiated until at least three reducing equivalents are present *(42)*. They further hypothesized that these "stored" reducing equivalents may be utilized for catalysis under conditions where electron transfer from the NrfA redox partner becomes sluggish, and that these stored electrons are replenished when the rate of electron transfer exceeds the diffusion of nitrite to the active site. Thus, Sosa *et al*. concluded that the extra hemes in NrfA function not only as a "wire" to transfer electrons to the active site, but that they can also serve as electron storage units *(42)*.

Given the structural arrangement of the hemes (Figure 3) and the proposed role for hemes 4 and 5 described above, it seems highly likely that heme 2 is the entry point for the incoming electrons *(26, 27)*. Furthermore, because hemes 2 and 3 in *G. lovleyi* NrfA have very similar midpoint potentials, it appears that these two hemes act as a biological wire that delivers electrons first to hemes 4 and 5 and then to heme 1 to initiate catalysis (Figure 4). In this scenario, heme 3 is at the nexus of this delivery network, and it has been proposed that one key role of heme 3 is to act as an electron gatekeeper, partitioning electrons between the active site

heme and the storage hemes *(42)*. Thus, any alteration that impacts the midpoint potential of heme 3 is likely to affect the catalytic efficiency.

This prediction was tested with a H108M variant in which the distal His of heme 3 was replaced with Met. As expected, the activity of H108M was significantly impaired, exhibiting <1% activity relative to the WT enzyme *(42)*. This substitution not only significantly shifts the heme 3 redox potential (becoming the most oxidizing of the 5 hemes), the H108M substitution also alters the midpoint potentials of the other hemes (Table 3), causing a rather complex change in the voltammogram. This observation provides further evidence for substantial electronic/electrostatic coupling between the various heme cofactors of NrfA.

Mechanism

Role of second-sphere active site residues

It is well established that NrfA can catalyze not only the reduction of nitrite, but also the reduction of nitric oxide (NO) and hydroxylamine (H_2NOH) *(14, 18, 25, 49-52)*. For all three of these substrates, ammonium was found to be the sole product. Based on these observations, it was proposed that NO and H_2NOH are plausible intermediates of the NrfA catalytic mechanism. The conversion of nitrite to ammonium by NrfA is facilitated by the presence of strictly conserved second coordination sphere residues at the active site, *i.e.*, glutamine, tyrosine, histidine, and arginine (distinct from the arginine that replaces calcium in some organisms, and this strictly conserved arginine is therefore hereafter referred to as Arg2 to avoid confusion) (Figure 6). Glutamine does not appear to have a significant role in the catalytic mechanism per se, as its substitution to glutamate did not affect V_{max}. The Gln → Glu substitution did, however,

lead to an increase in K_M, suggesting that the glutamine plays an important role in increasing the affinity of the enzyme for nitrite (Table 4) *(53)*.

Table 4. Conserved NrfA active site residues, their hypothesized functions, tested mutations, and the resulting effects.

Amino Acid	Substitution	Effect	Hypothesized Function	Organisms
Glutamine	Glutamate	Did not affect V_{max}; increased K_M	Increases the affinity of the enzyme for nitrite and proton delivery	*E. coli (53)*
			Tuning the pK_a values of the proton-coupled redox steps	
Tyrosine	Phenylalanine	Lost 99% of nitrite reduction activity; could still reduce sulfite	Proton delivery	*D. desulfuricans (34)*; *W. succinogenes (54)*; DFT studies *(55)*
			Tuning the pK_a values of the proton-coupled redox steps	
			Electron transfer, although highly unlikely	
Histidine	Asparagine	Could not reduce nitrite; could still reduce hydroxylamine	Proton delivery in earlier steps of the reaction	*D. desulfuricans (34)*; *E. coli* and *W. succinogenes (17)*
			Tuning the pK_a values of the proton-coupled redox steps	
			Substrate binding	
Arginine (Arg2)	Glutamine	Increased K_M, shifted the redox potential of a proton-coupled redox step	Substrate binding possibly through charge-charge interaction	*S. oneidensis (56)*
	Lysine	No change in K_M, shifted the redox potential of a proton-coupled redox step	May influence the midpoint potential of heme 1	
			Proton delivery	

Similarly, an Arg2 → Gln substitution in *Shewanella oneidensis* NrfA also led to a significant increase in K_M, suggesting that Arg2 is important for substrate binding as well,

possibly via a charge-charge interaction with the substrate (Table 4) *(56)*. This hypothesis was based on the observation that the corresponding Arg2 → Lys substitution had a smaller effect on the K_M of the enzyme than the Arg2 → Gln substitution. Both Arg2 → Lys and Arg2 → Gln substitutions greatly changed the pH electrocatalytic profile and the current-potential profile of the enzyme. These observations suggest that the conserved Arg2 plays a role in tuning the proton-coupled steps of the reaction at the active site *(56)*. Furthermore, the glutamine together with the active site histidine and tyrosine are proposed to be involved in proton delivery *(23, 24, 36)* and/or tuning the proton-coupled redox steps *(56)*.

Another potential role proposed for the conserved second coordination sphere tyrosine is as an electron donor *(23, 57)* as observed in other redox-active enzymes, including mammalian cysteine dioxygenase and photosystem II *(58-60)*. DFT calculations by Bykov *et al*. *(36, 55)*, however, do not support this role for tyrosine in NrfA due to the production of unstable intermediates and/or high energetic barriers. The active site tyrosine residue is likely a proton donor in the last step of the reaction. Figure 7 presents the mechanistic insights for each step of the NrfA nitrite to ammonium conversion based on experimental and theoretical investigations from Bykov *et al. (36)*.

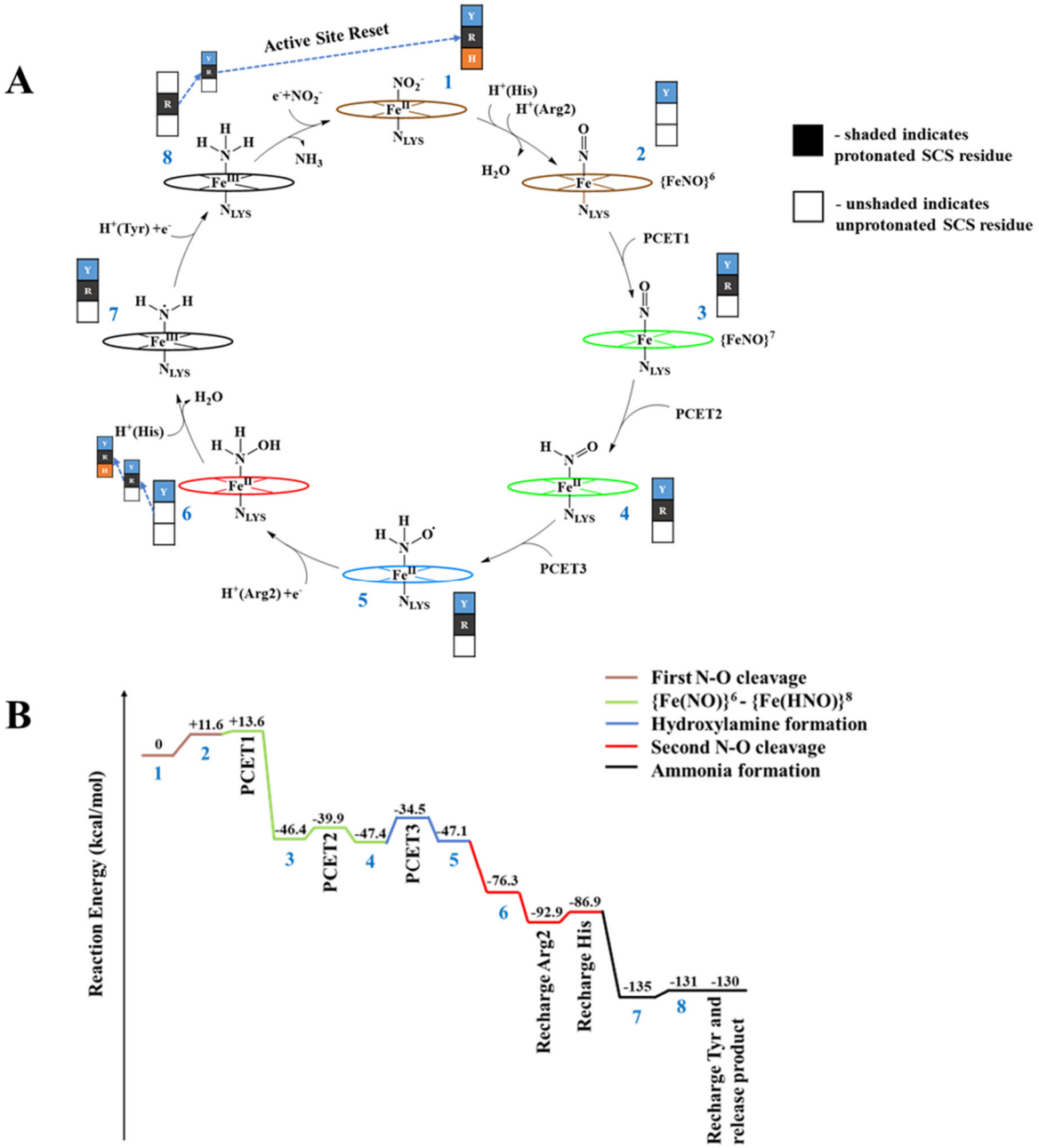

Figure 7. Summary of the theoretical calculations performed by Bykov et al. *(36)*. Panel A: Theoretical reaction cycle of nitrite reduction intermediates. The intermediate numbering and coloring correspond with panel B intermediates. The proton transfers with parenthetical 'His,' 'Arg2,' and 'Tyr' indicate which second coordination sphere (SCS) residue donates the proton. The stoplight-like boxes indicate the protonation state of the SCS residues at each intermediate step. The dashed arrows connecting the smaller boxes indicate SCS residue recharging, without a change in the chemical composition of the active site intermediate. Panel B: reaction energy diagram of the reaction cycle intermediates and SCS residue re-protonation. The y-axis indicates the free energy required for each reaction step. Panel B was adapted from reference *(36)*.

Reduction of NO_2^- to NO

In the resting state of the enzyme, heme 1 is in the high-spin configuration as revealed by EPR spectroscopy and magnetic circular dichroism *(41, 42, 44, 45)*, with the substrate binding site occupied by water *(25-27, 32, 53)*. The water molecule is labile and, based on DFT calculations, has an estimated binding energy of only -5.6 kcal/mol after heme 1 is reduced *(36, 61)*, thereby allowing the water to be readily displaced by nitrite. Nitrite binds to the heme iron via its N-atom after a one-electron reduction of the active site (Figure 7, intermediate **1**), and the binding of this strong-field ligand has been characterized and causes the active site heme to transition into a low-spin configuration *(23, 35, 44, 54, 62, 63)*. The nitrite is presumably stabilized not only through a H-bonding network with the active site Tyr, His, and Arg2 residues, but also through the π-backbonding interaction of the ferrous *d* metal orbitals with the nitrite lowest unoccupied molecular orbital (LUMO) (Figure 8). This π-backbonding, which is greater when the Fe is in the ferrous state *(23, 36, 54)*, also plays an important role in the activation of nitrite, *i.e.*, the N-O bond becomes weaker because of the partial electron transfer into the N-O π-antibonding LUMO of nitrite.

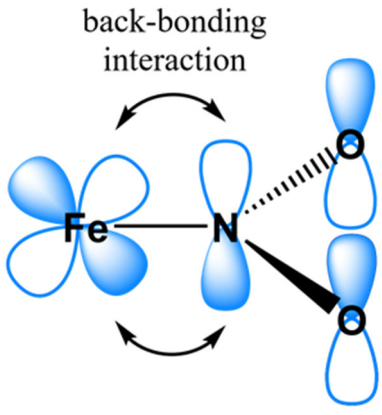

Figure 8. Heme 1 π-back-bonding interaction shown between the substrate, nitrite, and the Fe. Figure adapted from reference *(23)*.

Preliminary investigations of electron movement through the reaction cycle by Butt and coworkers *(50)* were later interpreted as one-electron stoichiometries for the reduction steps of the reaction *(64)*. Their conclusion was later supported by Judd *et al*. studying reductions of *S. oneidensis* NrfA *(14, 56)*. In the first step of the reaction, the cleavage of the nitrite N-O bond is predicted by theory to be a heterolytic process forming the low-spin (ls)-$\{Fe(NO)\}^6$ species[1] (Figure 7, Intermediate **2**) and water, as opposed to a homolytic cleavage mechanism which would lead to a ls-$\{Fe(NO)\}^7$ species and a $^{\bullet}OH$ radical *(23, 36)*. Experimentally, however, traces of a ls-$\{Fe(NO)\}^7$ species have been reported at this step *(45, 65)*.

The second step takes the ls-$\{Fe(NO)\}^6$ to a ls-$\{Fe(NO)\}^7$ intermediate in a proton coupled electron transfer (PCET) step. Because the ls-$\{Fe(NO)\}^7$ complex is a thermodynamically stable species whose formation is a potential kinetic trap for NrfA *(23)*, it might seem to be an unlikely catalytic intermediate. Ali *et al. (45)*, however, argued based on their computational investigations and rapid-mixing experiments that the rate-limiting step of the entire process is the reduction of the H_2NOH intermediate to ammonia. Therefore, any strong reductant that can overcome this rate-limiting step should be able to overcome the ls-$\{Fe(NO)\}^7$ thermodynamic stability. In addition, Bykov *et al.* found that an intermediate best described as ls-$\{Fe(NO)\}^7H_YH_R$, (Figure 7, Intermediate **3**), where H_Y and H_R denote protonation of the active site Tyr and Arg2, respectively, can readily undergo a proton-coupled electron transfer and become reduced to a Fe(II)-HNO species ($Fe^{II}(HNO)H_YH_R$ or Intermediate **4**) as discussed in the next section *(36)*.

[1]Enemark-Feltham notation: the exponent denotes the number of valence electrons, which includes the total number of *d* electrons on the Fe plus the NO(π*) electrons.

Finally, the active site histidine appears to assist the nitrite N-O cleavage *(17)*. This conclusion is based on the fact that the *E. coli* NrfA H264N variant catalyzes H_2NOH reduction at a similar rate as the wild-type enzyme, but the H264N variant is inactive towards nitrite reduction despite the oxidized form of the variant being able to bind the substrate with a $K_d = 48$ μM. Given that H264N still binds nitrite but does not allow nitrite reduction, the authors hypothesized that two of the roles of the histidine residue are to ensure the proper orientation of nitrite needed for reductive N-O bond cleavage and to facilitate proton transfer *(17)*. Based on crystal structures of *Wolinella succinogenes* and *Thioalkalivibrio nitratireducens* NrfAs, nitrite also forms H-bonds with the active site histidine *(23, 35, 54)*. In addition, a theoretical investigation suggested that a charged His can be an effective proton donor with a barrier of only +4.9 kcal/mol for the first proton transfer *(36)*. The second proton transfer to the substrate was found to be endothermic, regardless of which residue it came from. Under these conditions, proton transfer could be facilitated by Arg2, a re-protonated His, and/or a water molecule *(36)*. We have chosen to depict the second protonation event as a donation from Arg2 *(66)*, with the understanding that due to the similar energy barriers, the reaction could proceed via any of the mentioned donors.

Reduction of NO to HNO and then to H_2NOH

The reduction of NO by NrfA is well established both *in vivo (67-70)* and *in vitro (18, 49, 52)*, suggesting that NO is a plausible intermediate. Further theoretical investigations support this hypothesis *(23, 36)*. According to the DFT calculations by Bykov *et al. (36)*, the ls-$\{Fe(NO)\}^7$ species undergoes another PCET to form a species best described as a ls-Fe(II)-HNO complex (Figure 7, Intermediate **4**) *(36, 71)*. Analogous Fe(II)-HNO species have been observed in model

systems *(72-74)*, and evidence for such species has also been reported following the reduction of a myoglobin-nitrite complex *(75)*. $Fe^{II}(H_2NO^{\cdot})$ (Figure 7, Intermediate **5**) is hypothesized to form after a third PCET of the Fe^{II}(HNO) species, which then accepts a proton from Arg2 and undergoes an exothermic reduction to form a Fe-H_2NOH species (Figure 7, Intermediate **6**), discussed in more detail in the next section.

H_2NOH to NH_4^+ and product release

Like NO, H_2NOH can be reduced directly by NrfA *(14, 48-50, 70, 76, 77)*, and a crystal structure of oxidized NrfA with bound H_2NOH has been obtained *(23)*. Although the binding for H_2NOH is weaker (higher K_M) than the binding for both NO_2^- and NO, the *in vitro* turnover number for H_2NOH is the highest among the three substrates (highest k_{cat}) *(49, 70)*. Surprisingly, in the presence of high concentrations of H_2NOH but the absence of an exogenous reductant, fully oxidized NrfA only converts H_2NOH back to nitrite despite the more favorable thermodynamics of disproportionation of H_2NOH to ammonium and nitrite *(48)*.

Theoretical investigations by Bykov *et al*. *(36)* suggest that the H_2NOH to ammonia conversion involves protonation of each of the second coordination sphere residues, tyrosine, Arg2, and histidine, forming H-bonds to H_2NOH. These events are then followed by an intramolecular proton transfer from histidine which results in cleavage of the N-O bond, leading to the release of water and the transient formation of a formally Fe(II)-H_2N^+ complex. This species quickly obtains an electron from the iron, creating a Fe(III)-$H_2N^{\bullet}$ radical (Figure 7, Intermediate **7**). This intermediate is subsequently protonated to $NH_3^{\bullet}$ by the active site tyrosine and immediately reduced to NH_3 (Figure 7, Intermediate **8**). This tyrosine was found experimentally to be necessary for nitrite reduction activity *(54)*, although the first time this

conserved residue participates directly in the reaction mechanism appears to be during the last protonation step, according to the calculations.

Lastly, for the dissociation of the product from the active site, the tyrosine must first be re-protonated which decreases the energy barrier of the heme iron transitioning from a low-spin state to a high-spin state *(55)*. In the high-spin state, the product readily dissociates from the active site as it is now weakly bound to the heme *(55)*. The empty active site heme is now in a high-spin Fe(III) state. To restart the cycle, an electron reduces the heme iron to the ferrous state and nitrite can bind again.

Final Perspective

The presence of multiple hemes in cytochrome *c* nitrite reductase along with its fast kinetics make this enzyme very challenging to interrogate mechanistically. Thus, it is perhaps not surprising that it took nearly 30 years before the first putative intermediate, ls-{Fe(NO)}^{7}, was spectroscopically interrogated *(45)*, although the exact spectroscopic properties of this intermediate are still elusive. No other intermediate of the reaction cycle has been observed, leaving the catalytic mechanism of NrfA nebulous. A promising strategy for trapping plausible reaction intermediates of NrfA is to slow the enzyme kinetics, potentially by using an active site CXXCK → CXXCH variant or variants that slow down proton transfer to the active site. A key requirement for fast catalysis in NrfA is a perfectly orchestrated proton transfer mechanism, which, once it is better understood, could be interrupted to slow down catalysis and potentially trap intermediates. The CXXCK → CXXCH variant has been shown to have a specific activity that is 40% compared to that of the WT enzyme *(78)*. An additional advantage of employing the

CXXCK → CXXCH variant is that it may also help shed light on the functional role of the heme 1 lysine ligand.

Another challenge of interrogating the NrfA reaction mechanism is the non-discrete distribution of electrons among the hemes. In other words, one equivalent of electrons appears to be distributed over more than one heme, presumably because of the hemes' very close redox potentials. Careful simulation of the spectroscopic data in conjunction with precise electrochemical techniques such as cyclic voltammetry can enable researchers to overcome this challenge and better understand the complex electronic structures *(42)*. Substrate labeling experiments and the use of resonance Raman, electron-nuclear double resonance (ENDOR), as well as electron spin-echo envelope modulation (ESEEM) may prove to be very useful in providing mechanistic insights for NrfA.

Data Availability: The data cited in this review article are openly available in the provided references.

Acknowledgments: This material is based upon work supported by the U.S. Department of Energy, Office of Science, Basic Energy Sciences, under Award Number DE-SC0017952 (to E.L.H.) and DE-SC0018173 (to N.L.). This material is also based on work supported by the National Science Foundation Graduate Research Fellowship Program under Grant No. 2235783 (to K.H.). Any opinions, findings, and conclusions or recommendations expressed in this material are those of the author(s) and do not necessarily reflect the views of the National Science Foundation.

References:

([1.) Bowles, T. M., Atallah, S. S., Campbell, E. E., Gaudin, A., Wieder, W. R., and Grandy, A. S. (**2018**) Addressing agricultural nitrogen losses in a changing climate, *Nat. Sustain. 1*, 399-408.

([2.) Robertson, G. P., and Vitousek, P. M. (**2009**) Nitrogen in agriculture: balancing the cost of an essential resource, *Annu. Rev. Environ. Resour. 34*, 97-125.

([3.) Lassaletta, L., Billen, G., Grizzetti, B., Anglade, J., and Garnier, J. (**2014**) 50 year trends in nitrogen use efficiency of world cropping systems: the relationship between yield and nitrogen input to cropland, *Environ. Res. Lett. 9*, e105011.

([4.) Mosier, S., Cordova, S. C., and Robertson, G. P. (**2021**) Restoring Soil Fertility on Degraded Lands to Meet Food, Fuel, and Climate Security Needs via Perennialization, *Front. Sustain. Food Syst. 5*, e706142.

([5.) Popkin, G., Coruzzi, G., Hegg, E. L., Seefeldt, L., Stein, L., and Lehnert, N. (2015) Feeding the World in the 21st Century: Grand Challenges in the Nitrogen Cycle, National Science Foundation.

([6.) Cao, W., Yang, J., Li, Y., Liu, B., Wang, F., and Chang, C. (**2016**) Dissimilatory nitrate reduction to ammonium conserves nitrogen in anthropogenically affected subtropical mangrove sediments in Southeast China, *Mar. Pollut. Bull. 110*, 155-161.

([7.) Fernandes, S. O., Bonin, P. C., Michotey, V. D., Garcia, N., and LokaBharathi, P. A. (**2012**) Nitrogen-limited mangrove ecosystems conserve N through dissimilatory nitrate reduction to ammonium, *Sci. Rep. 2*, e419.

([8.) Pandey, C. B., Kumar, U., Kaviraj, M., Minick, K. J., Mishra, A. K., and Singh, J. S. (**2020**) DNRA: A short-circuit in biological N-cycling to conserve nitrogen in terrestrial ecosystems, *Sci. Total Environ. 738*, e139710.

([9.) Burgin, A. J., and Hamilton, S. K. (**2007**) Have we overemphasized the role of denitrification in aquatic ecosystems? A review of nitrate removal pathways, *Front. Ecol. Environ. 5*, 89-96.

([10.) Francis, C. A., Beman, J. M., and Kuypers, M. M. M. (**2007**) New processes and players in the nitrogen cycle: the microbial ecology of anaerobic and archaeal ammonia oxidation, *ISME J. 1*, 19-27.

([11.) Einsle, O. (**2011**) Structure and Function of Formate-Dependent Cytochrome *c* Nitrite Reductase, NrfA, *Meth. Enzymol. 496*, 399-422.

([12.) Kraft, B., Strous, M., and Tegetmeyer, H. E. (**2011**) Microbial nitrate respiration - Genes, enzymes and environmental distribution, *J. Biotech. 155*, 104-117.

([13.) Kroneck, P. M. H. (**2022**) Nature's nitrite-to-ammonia expressway, with no stop at dinitrogen, *J. Biol. Inorg. Chem. 27*, 1-21.

([14.) Judd, E. T., Youngblut, M., Pacheco, A. A., and Elliott, S. J. (**2012**) Direct electrochemistry of *Shewanella oneidensis* cytochrome *c* nitrite reductase: evidence of interactions across the dimeric interface, *Biochemistry 51*, 10175–10185.

([15.) Mohan, S. B., Schmid, M., Jetten, M., and Cole, J. (**2004**) Detection and widespread distribution of the *nrfA* gene encoding nitrite reduction to ammonia, a short circuit in the biological nitrogen cycle that competes with denitrification, *FEMS Microbiol. Ecol. 49*, 433-443.

([16.) Campeciño, J., Lagishetty, S., Wawrzak, Z., Alfaro, V.S., Lehnert, N., Reguera, G., Hu, J. and Hegg, E.L. (**2020**) Cytochrome *c* nitrite reductase from the bacterium *Geobacter lovleyi* represents a new NrfA subclass, *J. Biol. Chem. 295*, 11455-11465.

([17.) Lockwood, C. W., Burlat, B., Cheesman, M. R., Kern, M., Simon, J., Clarke, T. A., Richardson, D. J., and Butt, J. N. (**2015**) Resolution of Key Roles for the Distal Pocket Histidine in Cytochrome *c* Nitrite Reductases, *J. Am. Chem. Soc. 137*, 3059-3068.

([18.) Stach, P., Einsle, O., Schumacher, W., Kurun, E., and Kroneck, P. M. (**2000**) Bacterial cytochrome *c* nitrite reductase: new structural and functional aspects, *J. Inorg. Biochem. 79*, 381-385.

([19.) Silveira, C. M., Besson, S., Moura, I., Moura, J. J., and Almeida, M. G. (**2010**) Measuring the Cytochrome Nitrite Reductase Activity—Practical Considerations on the Enzyme Assays, *Bioinorg. Chem. Appl. 2010*, e1-8.
([20.) Simon, J. (**2002**) Enzymology and bioenergetics of respiratory nitrite ammonification, *FEMS Microbiol. Rev. 26*, 285-309.
([21.) Simon, J., Gross, R., Einsle, O., Kroneck, P. M. H., Kröger, A., and Klimmek, O. (**2000**) A NapC/NirT-type cytochrome *c* (NrfH) is the mediator between the quinone pool and the cytochrome *c* nitrite reductase of *Wolinella succinogenes*, *Mol. Microbiol. 35*, 686-696.
([22.) Beckett, C. S., Loughman, J. A., Karberg, K. A., Donato, G. M., Goldman, W. E., and Kranz, R. G. (**2000**) Four genes are required for the system II cytochrome *c* biogenesis pathway in *Bordetella pertussis*, a unique bacterial model, *Mol. Microbiol. 38*, 465-481.
([23.) Einsle, O., Messerschmidt, A., Huber, R., Kroneck, P. M., and Neese, F. (**2002**) Mechanism of the six-electron reduction of nitrite to ammonia by cytochrome *c* nitrite reductase, *J. Am. Chem. Soc. 124*, 11737-11745.
([24.) Einsle, O., Messerschmidt, A., Stach, P., Bourenkov, G. P., Bartunik, H. D., Huber, R., and Kroneck, P. M. (**1999**) Structure of cytochrome *c* nitrite reductase, *Nature 400*, 476-480.
([25.) Bamford, V. A., Angove, H. C., Seward, H. E., Thomson, A. J., Cole, J. A., Butt, J. N., Hemmings, A. M., and Richardson, D. J. (**2002**) Structure and spectroscopy of the periplasmic cytochrome *c* nitrite reductase from *Escherichia coli*, *Biochemistry 41*, 2921-2931.
([26.) Rodrigues, M. L., Oliveira, T. F., Pereira, I. A., and Archer, M. (**2006**) X-ray structure of the membrane-bound cytochrome *c* quinol dehydrogenase NrfH reveals novel haem coordination, *EMBO J. 25*, 5951-5960.
([27.) Einsle, O., Stach, P., Messerschmidt, A., Simon, J., Kroger, A., Huber, R., and Kroneck, P. M. (**2000**) Cytochrome *c* nitrite reductase from *Wolinella succinogenes*: structure at 1.6 Å resolution, inhibitor binding, and heme-packing motifs, *J. Biol. Chem. 275*, 39608-39616.
([28.) Youngblut, M., Judd, E. T., Srajer, V., Sayyed, B., Goelzer, T., Elliott, S. J., Schmidt, M., and Pacheco, A. A. (**2012**) Laue crystal structure of *Shewanella oneidensis* cytochrome *c* nitrite reductase from a high-yield expression system, *J. Biol. Inorg. Chem. 17*, 647-662.
([29.) Denkhaus, L., Siffert, F., and Einsle, O. (**2023**) An unusual active site architecture in cytochrome *c* nitrite reductase NrfA-1 from *Geobacter metallireducens*, *FEMS Microbiol. Lett. 370*, e1-8.
([30.) Lehnert, N., Kim, E., Dong, H. T., Harland, J. B., Hunt, A. P., Manickas, E. C., Oakley, K. M., Pham, J., Reed, G. C., and Alfaro, V. S. (**2021**) The Biologically Relevant Coordination Chemistry of Iron and Nitric Oxide: Electronic Structure and Reactivity, *Chem. Rev. 121*, 14682–14905.
([31.) Almeida, M. G., Macieira, S., Gonçalves, L. L., Huber, R., Cunha, C. A., Romao, M. J., Costa, C., Lampreia, J., Moura, J. J. G., and Moura, I. (**2003**) The isolation and characterization of cytochrome *c* nitrite reductase subunits (NrfA and NrfH) from *Desulfovibrio desulfuricans* ATCC 27774, *Eur. J. Biochem. 270*, 3904-3915.
([32.) Burlat, B., Gwyer, J., Poock, S., Clarke, T., Cole, J., Hemmings, A., Cheesman, M., Butt, J., and Richardson, D. (**2005**) Cytochrome *c* nitrite reductase: from structural to physicochemical analysis, *Biochem. Soc. Trans. 33*, 137-140.
([33.) Doyle, R. M., Marritt, S. J., Gwyer, J. D., Lowe, T. G., Tikhonova, T. V., Popov, V. O., Cheesman, M. R., and Butt, J. N. (**2013**) Contrasting catalytic profiles of multiheme nitrite reductases containing CxxCK heme-binding motifs, *J. Biol. Inorg. Chem. 18*, 655-667.
([34.) Cunha, C. A., Macieira, S., Dias, J. M., Almeida, G., Goncalves, L. L., Costa, C., Lampreia, J., Huber, R., Moura, J. J., Moura, I., and Romao, M. J. (**2003**) Cytochrome *c* nitrite reductase from *Desulfovibrio desulfuricans* ATCC 27774: the relevance of the two calcium sites in the structure of the catalytic subunit (NrfA), *J. Biol. Chem. 278*, 17455-17465.

([35.) Polyakov, K. M., Boyko, K. M., Tikhonova, T. V., Slutsky, A., Antipov, A. N., Zvyagilskaya, R. A., Popov, A. N., Bourenkov, G. P., Lamzin, V. S., and Popov, V. O. (**2009**) High-resolution structural analysis of a novel octaheme cytochrome *c* nitrite reductase from the haloalkaliphilic bacterium *Thioalkalivibrio nitratireducens*, *J. Mol. Biol. 389*, 846-862.
([36.) Bykov, D., and Neese, F. (**2015**) Six-electron reduction of nitrite to ammonia by cytochrome *c* nitrite reductase: insights from density functional theory studies, *Inorg. Chem. 54*, 9303-9316.
([37.) Clarke, T. A., Cole, J. A., Richardson, D. J., and Hemmings, A. M. (**2007**) The crystal structure of the pentahaem *c*-type cytochrome NrfB and characterization of its solution-state interaction with the pentahaem nitrite reductase NrfA, *Biochemistry 406*, 19-30.
([38.) Clarke, T. A., Dennison, V., Seward, H. E., Burlat, B., Cole, J. A., Hemmings, A. M., and Richardson, D. J. (**2004**) Purification and spectropotentiometric characterization of *Escherichia coli* NrfB, a decaheme homodimer that transfers electrons to the decaheme periplasmic nitrite reductase complex, *J. Biol. Chem. 279*, 41333-41339.
([39.) Lockwood, C., Butt, J. N., Clarke, T. A., and Richardson, D. J. (**2011**) Molecular interactions between multihaem cytochromes: probing the protein-protein interactions between pentahaem cytochromes of a nitrite reductase complex, *Biochem. Soc. T. 39*, 263-268.
([40.) Marritt, S. J., Kemp, G. L., Xiaoe, L., Durrant, J. R., Cheesman, M. R., and Butt, J. N. (**2008**) Spectroelectrochemical characterization of a pentaheme cytochrome in solution and as electrocatalytically active films on nanocrystalline metal-oxide electrodes, *J. Am. Chem. Soc. 130*, 8588-8589.
([41.) Stein, N., Love, D., Judd, E. T., Elliott, S. J., Bennett, B., and Pacheco, A. A. (**2015**) Correlations between the Electronic Properties of *Shewanella oneidensis* Cytochrome *c* Nitrite Reductase (ccNiR) and Its Structure: Effects of Heme Oxidation State and Active Site Ligation, *Biochemistry 54*, 3749-3758.
([42.) Sosa Alfaro, V., Campecino, J., Tracy, M., Elliott, S. J., Hegg, E. L., and Lehnert, N. (**2021**) Elucidating Electron Storage and Distribution within the Pentaheme Scaffold of Cytochrome *c* Nitrite Reductase (NrfA), *Biochemistry 60*, 1853-1867.
([43.) Berry, E. A., and Walker, F. A. (**2008**) Bis-histidine-coordinated hemes in four-helix bundles: how the geometry of the bundle controls the axial imidazole plane orientations in transmembrane cytochromes of mitochondrial complexes II and III and related proteins, *J. Biol. Inorg. Chem. 13*, 481-498.
([44.) Martins, G., Rodrigues, L., Cunha, F. M., Matos, D., Hildebrandt, P., Murgida, D. H., Pereira, I. A., and Todorovic, S. (**2010**) Substrate binding to a nitrite reductase induces a spin transition, *J. Phys. Chem. B. 114*, 5563-5566.
([45.) Ali, M., Stein, N., Mao, Y., Shahid, S., Schmidt, M., Bennett, B., and Pacheco, A. A. (**2019**) Trapping of a Putative Intermediate in the Cytochrome *c* Nitrite Reductase (ccNiR)-Catalyzed Reduction of Nitrite: Implications for the ccNiR Reaction Mechanism, *J. Am. Chem. Soc. 141*, 13358-13371.
([46.) Costa, C., Moura, J. J., Moura, I., Wang, Y., and Huynh, B. H. (**1996**) Redox properties of cytochrome *c* nitrite reductase from *Desulfovibrio desulfuricans* ATCC 27774, *J. Biol. Chem. 271*, 23191-23196.
([47.) Almeida, M. G., Silveira, C. M., Guigliarelli, B., Bertrand, P., Moura, J. J., Moura, I., and Leger, C. (**2007**) A needle in a haystack: the active site of the membrane-bound complex cytochrome *c* nitrite reductase, *FEBS Lett. 581*, 284-288.
([48.) Youngblut, M., Pauly, D. J., Stein, N., Walters, D., Conrad, J. A., Moran, G. R., Bennett, B., and Pacheco, A. A. (**2014**) *Shewanella oneidensis* cytochrome *c* nitrite reductase (ccNiR) does not disproportionate hydroxylamine to ammonia and nitrite, despite a strongly favorable driving force, *Biochemistry 53*, 2136-2144.

([49.) van Wonderen, J. H., Burlat, B., Richardson, D. J., Cheesman, M. R., and Butt, J. N. (**2008**) The nitric oxide reductase activity of cytochrome *c* nitrite reductase from *Escherichia coli*, *J. Biol. Chem. 283*, 9587-9594.
([50.) Angove, H. C., Cole, J. A., Richardson, D. J., and Butt, J. N. (**2002**) Protein film voltammetry reveals distinctive fingerprints of nitrite and hydroxylamine reduction by a cytochrome *c* nitrite reductase, *J. Biol. Chem. 277*, 23374-23381.
([51.) Berks, B. C., Ferguson, S. J., Moir, J. W. B., and Richardson, D. J. (**1995**) Enzymes and associated electron transport systems that catalyse the respiratory reduction of nitrogen oxides and oxyanions, *Biochim. Biophys. Acta Bioenerg. 1232*, 97-173.
([52.) Costa, C., Macedo, A., Moura, I., Moura, J. J., Le Gall, J., Berlier, Y., Liu, M. Y., and Payne, W. J. (**1990**) Regulation of the hexaheme nitrite/nitric oxide reductase of *Desulfovibrio desulfuricans*, *Wolinella succinogenes* and *Escherichia coli*: a mass spectrometric study, *FEBS Lett. 276*, 67-70.
([53.) Clarke, T. A., Kemp, G. L., Van Wonderen, J. H., Doyle, R. M., Cole, J. A., Tovell, N., Cheesman, M. R., Butt, J. N., Richardson, D. J., and Hemmings, A. M. (**2008**) Role of a conserved glutamine residue in tuning the catalytic activity of *Escherichia coli* cytochrome *c* nitrite reductase, *Biochemistry 47*, 3789-3799.
([54.) Lukat, P., Rudolf, M., Stach, P., Messerschmidt, A., Kroneck, P. M., Simon, J., and Einsle, O. (**2008**) Binding and reduction of sulfite by cytochrome *c* nitrite reductase, *Biochemistry 47*, 2080-2086.
([55.) Bykov, D., Plog, M., and Neese, F. (**2014**) Heme-bound nitroxyl, hydroxylamine, and ammonia ligands as intermediates in the reaction cycle of cytochrome *c* nitrite reductase: a theoretical study, *J. Biol. Inorg. Chem. 19*, 97-112.
([56.) Judd, E. T., Stein, N., Pacheco, A. A., and Elliott, S. J. (**2014**) Hydrogen bonding networks tune proton-coupled redox steps during the enzymatic six-electron conversion of nitrite to ammonia, *Biochemistry 53*, 5638-5646.
([57.) Trofimov, A. A., Polyakov, K. M., Tikhonova, T. V., Tikhonov, A. V., Safonova, T. N., Boyko, K. M., Dorovatovskii, P. V., and Popov, V. O. (**2012**) Covalent modifications of the catalytic tyrosine in octahaem cytochrome *c* nitrite reductase and their effect on the enzyme activity, *Acta Crystallogr. D. 68*, 144-153.
([58.) Driggers, C. M., Kean, K. M., Hirschberger, L. L., Cooley, R. B., Stipanuk, M. H., and Karplus, P. A. (**2016**) Structure-Based Insights into the Role of the Cys-Tyr Crosslink and Inhibitor Recognition by Mammalian Cysteine Dioxygenase, *J. Mol. Biol. 428*, 3999-4012.
([59.) Yachandra, V. K., Sauer, K., and Klein, M. P. (**1996**) Manganese cluster in photosynthesis: Where plants oxidize water to dioxygen, *Chem. Rev. 96*, 2927-2950.
([60.) Cox, N., Pantazis, D. A., and Lubitz, W. (**2020**) Current Understanding of the Mechanism of Water Oxidation in Photosystem II and Its Relation to XFEL Data, *Annu. Rev. Biochem. 89*, 795-820.
([61.) Bykov, D., and Neese, F. (**2011**) Substrate binding and activation in the active site of cytochrome *c* nitrite reductase: a density functional study, *J. Biol. Inorg. Chem. 16*, 417-430.
([62.) Pereira, I. A., LeGall, J., Xavier, A. V., and Teixeira, M. (**2000**) Characterization of a heme *c* nitrite reductase from a non-ammonifying microorganism, *Desulfovibrio vulgaris* Hildenborough, *Biochim. Biophys. Acta 1481*, 119-130.
([63.) Nilsson, Z. N., Mandella, B. L., Sen, K., Kekilli, D., Hough, M. A., Moenne-Loccoz, P., Strange, R. W., and Andrew, C. R. (**2017**) Distinguishing Nitro vs Nitrito Coordination in Cytochrome *c*' Using Vibrational Spectroscopy and Density Functional Theory, *Inorg. Chem. 56*, 13205-13213.
([64.) Gates, A. J., Kemp, G. L., To, C. Y., Mann, J., Marritt, S. J., Mayes, A. G., Richardson, D. J., and Butt, J. N. (**2011**) The relationship between redox enzyme activity and electrochemical potential-cellular and mechanistic implications from protein film electrochemistry, *Phys. Chem. Chem. Phys. 13*, 7720-7731.

([65.) Shahid, S., Ali, M., Legaspi-Humiston, D., Wilcoxen, J., and Pacheco, A. A. (**2021**) A Kinetic Investigation of the Early Steps in Cytochrome *c* Nitrite Reductase (ccNiR) - Catalyzed Reduction of Nitrite, *Biochemistry 60*, 2098-2115.
([66.) Bykov, D., and Neese, F. (**2012**) Reductive activation of the heme iron-nitrosyl intermediate in the reaction mechanism of cytochrome *c* nitrite reductase: a theoretical study, *J. Biol. Inorg. Chem. 17*, 741-760.
([67.) Poock, S. R., Leach, E. R., Moir, J. W., Cole, J. A., and Richardson, D. J. (**2002**) Respiratory detoxification of nitric oxide by the cytochrome *c* nitrite reductase of *Escherichia coli*, *J. Biol. Chem. 277*, 23664-23669.
([68.) Kern, M., Volz, J., and Simon, J. (**2011**) The oxidative and nitrosative stress defence network of *Wolinella succinogenes*: cytochrome *c* nitrite reductase mediates the stress response to nitrite, nitric oxide, hydroxylamine and hydrogen peroxide, *Environ. Microbiol. 13*, 2478-2494.
([69.) Clarke, T. A., Mills, P. C., Poock, S. R., Butt, J. N., Cheesman, M. R., Cole, J. A., Hinton, J. C., Hemmings, A. M., Kemp, G., Soderberg, C. A., Spiro, S., Van Wonderen, J., and Richardson, D. J. (**2008**) *Escherichia coli* cytochrome *c* nitrite reductase NrfA, *Methods Enzymol. 437*, 63-77.
([70.) Atkinson, S. J., Mowat, C. G., Reid, G. A., and Chapman, S. K. (**2007**) An octaheme *c*-type cytochrome from *Shewanella oneidensis* can reduce nitrite and hydroxylamine, *FEBS Lett. 581*, 3805-3808.
([71.) Goodrich, L. E., and Lehnert, N. (**2013**) The trans effect of nitroxyl (HNO) in ferrous heme systems: Implications for soluble guanylate cyclase activation by HNO, *J. Inorg. Biochem. 118*, 179-186.
([72.) Bonner, F. T., and Pearsall, K. A. (**1982**) Aqueous Nitrosyliron(II) Chemistry. 1. Reduction of Nitrite and Nitric-Oxide by Iron(II) and (Trioxodinitrato)iron(II) in Acetate Buffer. Intermediacy of Nitrosyl Hydride, *Inorg. Chem. 21*, 1973-1978.
([73.) Manickas, E. C., Lalonde, A. B., Hu, M. Y., Alp, E. E., and Lehnert, N. (**2023**) Stabilization of a Heme-HNO Model Complex Using a Bulky Bis-Picket Fence Porphyrin and Reactivity Studies with NO, *J. Am. Chem. Soc. 145*, 23014-23026.
([74.) Abucayon, E. G., Khade, R. L., Powell, D. R., Zhang, Y., and Richter-Addo, G. B. (**2016**) Hydride Attack on a Coordinated Ferric Nitrosyl: Experimental and DFT Evidence for the Formation of a Heme Model-HNO Derivative, *J. Am. Chem. Soc. 138*, 104-107.
([75.) Lin, R., and Farmer, P. J. (**2000**) The HNO adduct of myoglobin: Synthesis and characterization, *J. Am. Chem. Soc. 122*, 2393-2394.
([76.) Rudolf, M., Einsle, O., Neese, F., and Kroneck, P. M. (**2002**) Pentahaem cytochrome *c* nitrite reductase: reaction with hydroxylamine, a potential reaction intermediate and substrate, *Biochem. Soc. Trans. 30*, 649-653.
([77.) Gwyer, J. D., Angove, H. C., Richardson, D. J., and Butt, J. N. (**2004**) Redox-triggered events in cytochrome *c* nitrite reductase, *Bioelectrochemistry 63*, 43-47.
([78.) Pisa, R., Stein, T., Eichler, R., Gross, R., and Simon, J. (**2002**) The *nrfI* gene is essential for the attachment of the active site haem group of *Wolinella succinogenes* cytochrome *c* nitrite reductase, *Mol. Microbiol. 43*, 763-770.